ORIGINAL ARTICLE

Tryptanthrin attenuates TLR3-mediated STAT1 activation in THP-1 cells

Noriyuki Numao[1] · Shogo Kawaguchi[1] · Jiangli Ding[1] · Takao Karasawa[1,2] · Kazuhiko Seya[1] · Tomoh Matsumiya[3] · Hidezumi Kikuchi[4] · Hirotake Sakuraba[4] · Shinsaku Fukuda[4] · Tadaatsu Imaizumi[1]

Abstract

Upon viral infection, dysregulated immune responses are associated with the disease exacerbation and poor prognosis. The Janus kinase/signal transducers and activators of transcription (JAK/STAT) pathway are essential for the innate immune responses against invading viruses as well as for sustained activation of macrophages. Tryptanthrin, a natural alkaloid, exhibits various bioactivities, including anti-microbial and anti-inflammatory effects. The aim of this study was to elucidate the effects of tryptanthrin on toll-like receptor 3 (TLR3)–mediated STAT1 activation in macrophages in vitro. Using phorbol myristate acetate (PMA)–differentiated THP-1 cells, we analyzed the protein level of phosphorylated-STAT1 (p-STAT1) upon stimulation with polyinosinic-polycytidylic acid (poly IC), a well-known TLR3 ligand, with and without tryptanthrin. We found that tryptanthrin decreased the protein level of p-STAT1 in a concentration-dependent manner after poly IC stimulation. On the other hand, tryptanthrin did not affect the levels of p-STAT1 upon stimulation with lipopolysaccharide from *Escherichia coli*. Consistently, tryptanthrin suppressed poly IC–induced mRNA expression of interferon (IFN)–stimulated genes which are regulated by STAT1. Moreover, tryptanthrin decreased the protein level of phosphorylated-IFN regulatory factor 3 and the subsequent IFN-β mRNA induction after poly IC stimulation. Tryptanthrin is a promising therapeutic agent for the aberrant activation of macrophages caused by viral infection.

Keywords Tryptanthrin · THP-1 · Macrophages · Double-stranded RNA · STAT1

Introduction

Pattern recognition receptors (PRRs) play a key role in the innate immune responses against microorganisms. Antigen-presenting cells, such as macrophages and dendritic cells, recognize invading viruses through PRRs and activate innate immune responses. Toll-like receptor (TLR) 3 is localized on the endosomal membrane and recognizes viral double-stranded RNA (dsRNA) [1]. Binding of dsRNA to TLR3 leads to the phosphorylation of interferon regulatory factor (IRF) 3 and consequent type I interferon (IFN) induction [2]. Secreted type I IFN proteins bind to type I IFN receptors in an autocrine or paracrine manner, followed by IFN-stimulated response element (ISRE)–activated IFN-stimulated gene (ISG) transcription through the Janus kinase/signal transducers and activators of transcription 1 (JAK/STAT1) pathway [3]. STAT1 is an essential transcription factor for type I IFN signaling, and many ISGs function as direct inhibitors of viral proliferation as well as regulators of JAK/STAT signaling [4]. The canonical pathway of TLR3-mediated signaling is involved in innate immune responses against many types of viruses, including severe acute respiratory syndrome coronavirus 2 (SARS-CoV-2) [5].

The majority of patients infected with SARS-CoV-2 have a mild clinical manifestation, whereas some patients suffer from lethal pneumonia, acute respiratory distress syndrome (ARDS), and multiple organ failure, namely, severe coronavirus disease 2019 (COVID-19) [6]. It has been shown that type I IFN signaling plays a critical role in the rapid induction of antiviral immune responses against SARS-CoV-2, and type I IFN has therefore emerged as a potential therapeutic candidate

✉ Shogo Kawaguchi
kawaguchi.s@hirosaki-u.ac.jp

1 Department of Vascular Biology, Institute of Brain Science, Hirosaki University Graduate School of Medicine, 5 Zaifu-cho, Hirosaki, Aomori 036-8562, Japan

2 Department of Pediatrics, Hirosaki University Graduate School of Medicine, 5 Zaifu-cho, Hirosaki, Aomori 036-8562, Japan

3 Department of Bioscience and Laboratory Medicine, Hirosaki University Graduate School of Health Science, 5 Zaifu-cho, Hirosaki, Aomori 036-8564, Japan

4 Department of Gastroenterology and Hematology, Hirosaki University Graduate School of Medicine, 5 Zaifu-cho, Hirosaki, Aomori 036-8562, Japan

for COVID-19 [7]. Although appropriate activation of TLR3 signaling is important to eliminate viruses, the dysregulated immune responses may lead to the exacerbation of diseases. In fact, delayed IFN response and inflammatory macrophages cause lethal pneumonia in SARS-CoV-infected mice [8]. Moreover, the type I IFN response exacerbates proinflammatory cytokine–driven inflammation in patients with severe COVID-19 [9]. The expression of various ISGs is upregulated in peripheral blood mononuclear cells (PBMCs) from patients with severe COVID-19 [10], suggesting that dysregulated type I IFN responses may be associated with the hyper-inflammatory state in COVID-19. The JAK/STAT pathway is essential for regulating of type I IFN signaling, and the efficacy of a JAK inhibitor has been clinically studied in severe COVID-19 [11].

Tryptanthrin (indolo[2,1-*b*]quinazoline-6,12-dione) is a natural alkaloid isolated from indigo plants, such as *Polygonum tinctorium*. Tryptanthrin exhibits various biological activities, including antimicrobial and antiviral effects [12, 13]. We previously reported that tryptanthrin suppresses dsRNA-induced STAT1 phosphorylation in cultured human umbilical vein endothelial cells (HUVECs) [14]. However, it remains unknown whether tryptanthrin affects TLR3-mediated signaling in macrophages. In the present study, we focused on the immunomodulatory functions of tryptanthrin in TLR3 signaling in macrophages, and investigated dsRNA-induced STAT1 activation using phorbol myristate acetate (PMA)–differentiated THP-1-derived macrophage-like cells (THP-1 Mϕ). Additionally, we examined STAT-1-mediated mRNA expression of classical ISGs such as IFN-induced protein with tetratricopeptide repeats (IFIT) 1, IFIT2, myxovirus resistance protein 1 (Mx1), and IFN-induced transmembrane protein 1 (IFITM1).

Material and methods

Reagents

Tryptanthrin (purity 98%) and recombinant human IFN-β (rIFN-β) were purchased from Combi-Blockes, Inc. (San Diego, CA, USA) and PeproTech (Cranbury, NJ, USA), respectively. Polyinosinic-polycytidylic acid (poly IC), lipopolysaccharides (LPS) from *Escherichia coli*, and recombinant human IFN-γ (rIFN-γ) were obtained from Sigma-Aldrich (St. Louis, MO, USA). Rabbit monoclonal anti-phosphorylated IRF3 (p-IRF3) antibody (#4947) and rabbit polyclonal anti-phosphorylated STAT1 (Ser727) (p-STAT1-Ser) antibody (#9177) were obtained from Cell Signaling Technology (Danvers, MA, USA). Mouse monoclonal anti-IRF3 (sc-33641), rabbit polyclonal anti-STAT1 (sc-346), mouse monoclonal anti-p-STAT1 (pY701.4A) (p-STAT1-Tyr) (sc-136229), and mouse monoclonal anti-TLR3 (sc-32232) antibodies were purchased from Santa Cruz Biotechnology (Dallas, TX,

USA). Moloney murine leukemia virus (M-MLV) reverse transcriptase and oligo(dT)$_{18}$ were obtained from Invitrogen (Carlsbad, CA, USA). Mouse monoclonal anti-CD68 antibody (#14–0688), anti-TLR3 antibody (#14–9039), Alexa Fluor 488 anti-mouse immunoglobulin (Ig)G antibody (A11029), Alexa Fluor 594 anti-rabbit IgG antibody (A21207), and ProLong™ Gold antifade reagent with 4′,6-diamidino-2-phenylindole (DAPI) were purchased from Thermo Fisher Scientific (Rockford, IL, USA). Fluorescein isothiocyanate (FITC)–labeled goat anti-mouse IgG antibody (#SA00003-1) was purchased from Proteintech (Rosemont, IL, USA). The NucleoSpin RNA kit and Thunderbird™ Next SYBR® qPCR mix were purchased from Macherey–Nagel GmbH and Co. KG (Düren, Germany) and Toyobo (Osaka, Japan), respectively. BCA protein assay reagent was obtained from Pierce/Thermo Scientific Inc. (Waltham, MA, USA). Polyvinylidene fluoride (PVDF) membranes and Luminata Crescendo Western horseradish peroxidase (HRP) substrates were obtained from Millipore Corporation (Billerica, MA, USA). The intracellular cytokine staining kit was obtained from Becton Dickinson (San Jose, CA, USA).

Cell culture

THP-1, a human monocytic leukemia cell line, was cultured in Roswell Park Memorial Institute (RPMI) 1640 medium containing 10% fetal bovine serum (FBS), 100 mg/mL penicillin, and 100 mg/mL streptomycin at 37 °C under 5% CO_2. To differentiate THP-1 cells into THP-1 Mϕ, they were stimulated with 10 ng/mL PMA for 48 h. Under these conditions, more than 90% of cells were attached to the surface of culture dishes and the cell morphology changed to a "spindle-shape" (Fig. 1A). After an additional 24 h of incubation without PMA, the cells were stimulated using poly IC, LPS, rIFN-β, or rIFN-γ with or without 0.01–1 μM of tryptanthrin.

Quantitative real-time reverse transcription polymerase chain reaction (qRT-PCR)

Total RNA was extracted from the cells using the NucleoSpin RNA kit according to the manufacturer's instructions. Single-strand complementary DNA (cDNA) was synthesized using oligo (dT)$_{18}$ primers and M-MLV reverse transcriptase. qRT-PCR was performed using a Bio-Rad CFX real-time PCR thermocycler and Thunderbird™ Next SYBR® qPCR Mix. The results were normalized to glyceraldehyde 3-phosphate dehydrogenase (GAPDH) RNA. All assays were performed in triplicate. The primer sequences that were used are as follows: IFIT1-F: 5′-TAGCCAACATGTCCTCACAGAC-3′, IFIT1-R: 5′-TCTTCTACCACTGGTTTCATGC-3′; IFIT2-F: 5′-GGTCTCTTCAGCATTTATTGGTG-3′, IFIT2-R: 5′- TGCCGTAGGCTGCTCTCCA-3′; IFITM1-F: 5′-TCGCCTACTCCGTGAAGT
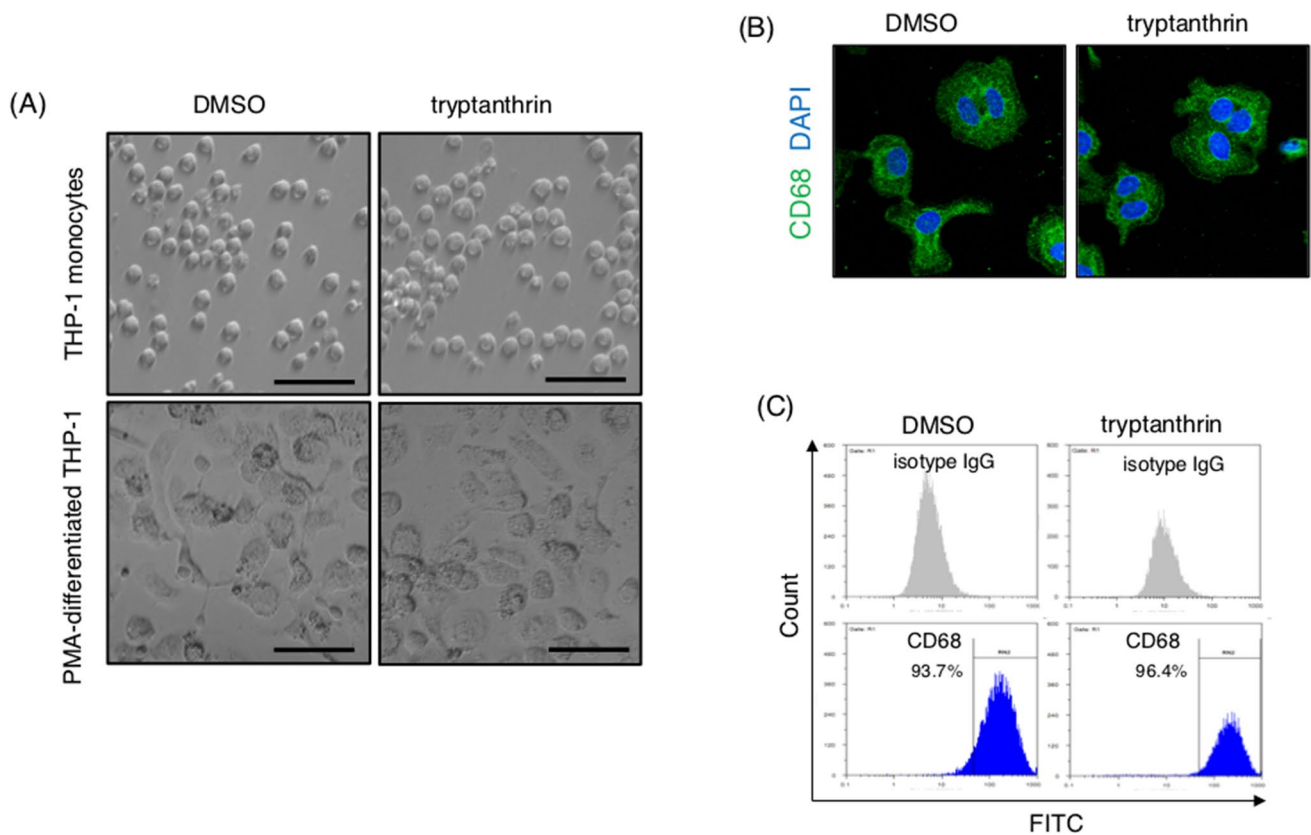
Fig. 1 A Representative bright-field images of THP-1 monocytes and phorbol myristate acetate (PMA)–differentiated THP-1 macrophage-like cells (THP-1 Mϕ) 24 h after treatment with 1 µM tryptanthrin or dimethylsulfoxide (DMSO). Scale bars represent 100 µm. **B** THP-1 Mϕ were incubated for 24 h with tryptanthrin or DMSO, and fixed with methanol. The cells were labeled with anti-CD68 antibody (green), and visualized using a confocal laser scanning microscope. Cell nuclei were stained with 4′,6-diamidino-2-phenylindole (DAPI) (blue). Representative images of three independent experiments. **C** Flow cytometry analysis of CD68 expression in THP-1 Mϕ stimulated with 1 µM tryptanthrin (right panel) or DMSO (left panel). Representative histograms of three to five independent experiments

CTA-3′, IFITM1-R: 5′-TGTCACAGAGCCGAATACCAG-3′; ISG15-F: 5′-GGCTGGGACCTGACGGTGAAG-3′, ISG15-R: 5′-GTCCGCCCGCCAGGCTCTGT-3′; Mx1-F: 5′-GCCAGGACCAGGTATACAG-3′, Mx1-R: 5′-GCCTGC GTCAGCCGTGC-3′; IFN-β-F: 5′-CCTGTGGCAATTGAA TGGGAGGC-3′, IFN-β-R: 5′-CCAGGCACAGTGACTGTA CTCCTT-3′; TLR3-F: 5′-TGTCTGGAAGAAAGGGAC TTTGA-3′, TLR3-R: 5′-GTTGAACTGCATGATGTACCT TGA-3′; tumor necrosis factor-α (TNF-α)-F: TGGCCTGCA ACTAATCAACC; TNF-α-R: GTGTGGAAGGACATC CTTGG; and GAPDH-F: 5′-GCACCGTCAAGGCTGAGA AC-3′; GAPDH-R: 5′-ATGGTGGTGAAGACGCCAGT-3′.

Western blotting

The cells were washed twice with phosphate-buffered saline (PBS), lysed with RIPA buffer containing 0.2% proteinase inhibitors, and centrifuged at 12,000 rpm for 10 min at 4 °C. Following this, the supernatants were collected. After determining protein concentration with BCA protein assay reagent, equal amounts of proteins were loaded on a 5–20% sodium dodecyl sulfate (SDS) polyacrylamide gel for electrophoresis. The separated proteins were transferred onto PVDF membranes. The membranes were blocked using Tris-buffered saline with Tween 20 (TBS-T, pH7.4) containing 5% nonfat dry milk or 5% bovine serum albumin, and incubated overnight at 4 °C with a primary antibody against p-STAT1-Ser, p-STAT1-Tyr, STAT1, p-IRF3, or IRF3. After incubating the membranes with HRP-conjugated secondary antibodies for 1 h at room temperature, visualization was performed using Luminata Crescendo substrate.

Immunofluorescence (IF)

PMA-differentiated THP-1 cells cultivated on 4-well chamber slides were incubated with 1µM tryptanthrin or dimethylsulfoxide (DMSO) for 24 h, and then fixed with

methanol. After blocking with 5% goat serum in PBS with Tween 20 (PBS-T) for 30 min, the cells were stained with a mouse anti-CD68 antibody (1:250) or a mouse anti-TLR3 antibody (1:250) overnight at 4 °C. Similarly, THP-1 Mφ were stimulated with poly IC or LPS for 2 h or 1 h, with and without tryptanthrin, and then fixed. After blocking with 5% goat or donkey serum in PBS-T for 30 min, the cells were stained with a mouse anti-STAT1 antibody (1:250) or a rabbit anti-IRF3 antibody (1:250). The cells were further stained with Alexa Fluor 488–conjugated goat anti-mouse IgG antibody (1:250) or Alexa Fluor 594–conjugated donkey anti-rabbit IgG antibody (1:250) for 1 h at room temperature, and the slides were mounted with ProLong Gold Antifade

Reagent. The cells were visualized using a confocal laser scanning microscope (C1si; Nikon, Tokyo, Japan).

Flow cytometry analysis

THP-1 cells were differentiated as described above and incubated with 1 µM tryptanthrin or DMSO for 24 h. The cells were detached from the culture plate using trypsin/EDTA (Nacalai tesque, Kyoto, Japan) and permeabilized with the Cytofix/Cytoperm buffer in the intracellular staining kit, according to the manufacturer's instructions. Cells were blocked using normal goat serum, and then stained with an anti-CD68 antibody, an anti-TLR3 antibody, or isotype mouse IgG1 for 30 min. After staining with FITC-labeled anti-mouse IgG
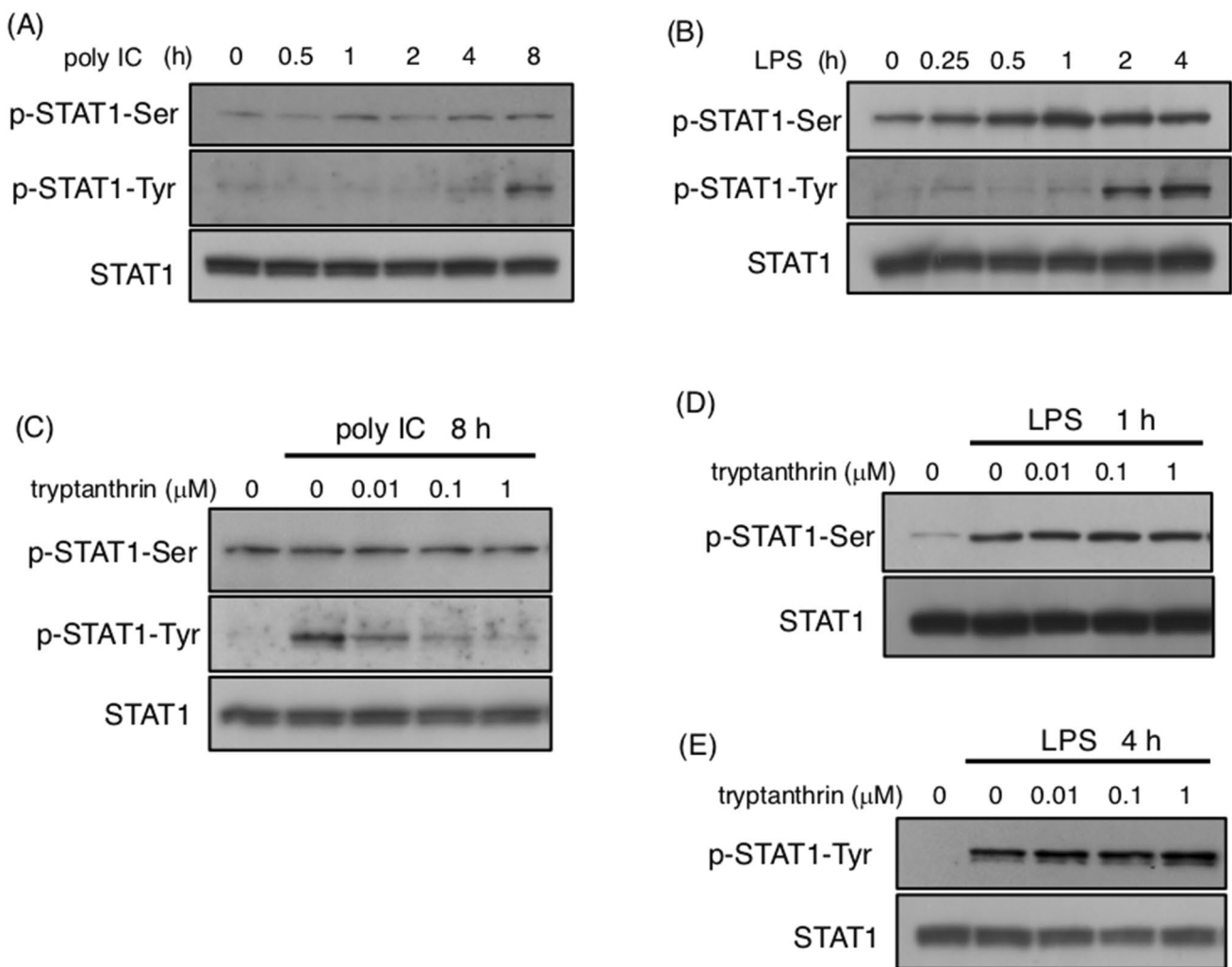

Fig. 2 A THP-1 Mφ were stimulated with 20 µg/mL polyinosinic-polycytidylic acid (poly IC) for 8 h. The cell lysates were subjected to western blotting to analyze the expression of p-STAT1-Ser, p-STAT1-Tyr, and STAT1. B Cells were stimulated using 1 µg/mL lipopolysaccharides (LPS) for 4 h. The cell lysates were subjected to western blotting to analyze the expression of p-STAT1-Ser, p-STAT1-Tyr, and STAT1. C Cells were stimulated with 20 µg/mL poly IC and 0.01–1 µM tryptanthrin for 8 h. The expression of p-STAT1-Ser, p-STAT1-Tyr, and STAT1 proteins was analyzed using western blotting. Cells were stimulated with 1 µg/mL LPS and 0.01–1 µM tryptanthrin, and the expression of p-STAT1-Ser (D) and p-STAT1-Tyr (E) was analyzed at 1 h and 4 h, respectively. Representative images of three independent experiments

antibody for 30 min, the cells were washed and resuspended in the stain buffer. Flow cytometric measurements were performed using CyFlow Space (Sysmex, Copenhagen, Denmark).

Statistical analysis

All data are presented as mean ± standard deviation (SD). Statistical differences were analyzed using a two-tailed *t*-test, Mann–Whitney *U* test, or one-way analysis of variance (ANOVA). Statistical significance was set at $p < 0.05$.

Results

Tryptanthrin decreases the levels of p-STAT1-Tyr after poly IC stimulation

First, we confirmed whether tryptanthrin could affect the morphology of both THP-1 monocytes and Mϕ. As shown in Fig. 1A, the morphology of THP-1 monocytes and Mϕ did not differ between the DMSO or tryptanthrin-treated cells. More than 90% of THP-1 Mϕ expressed CD68, a well-known marker for matured macrophages, and tryptanthrin treatment
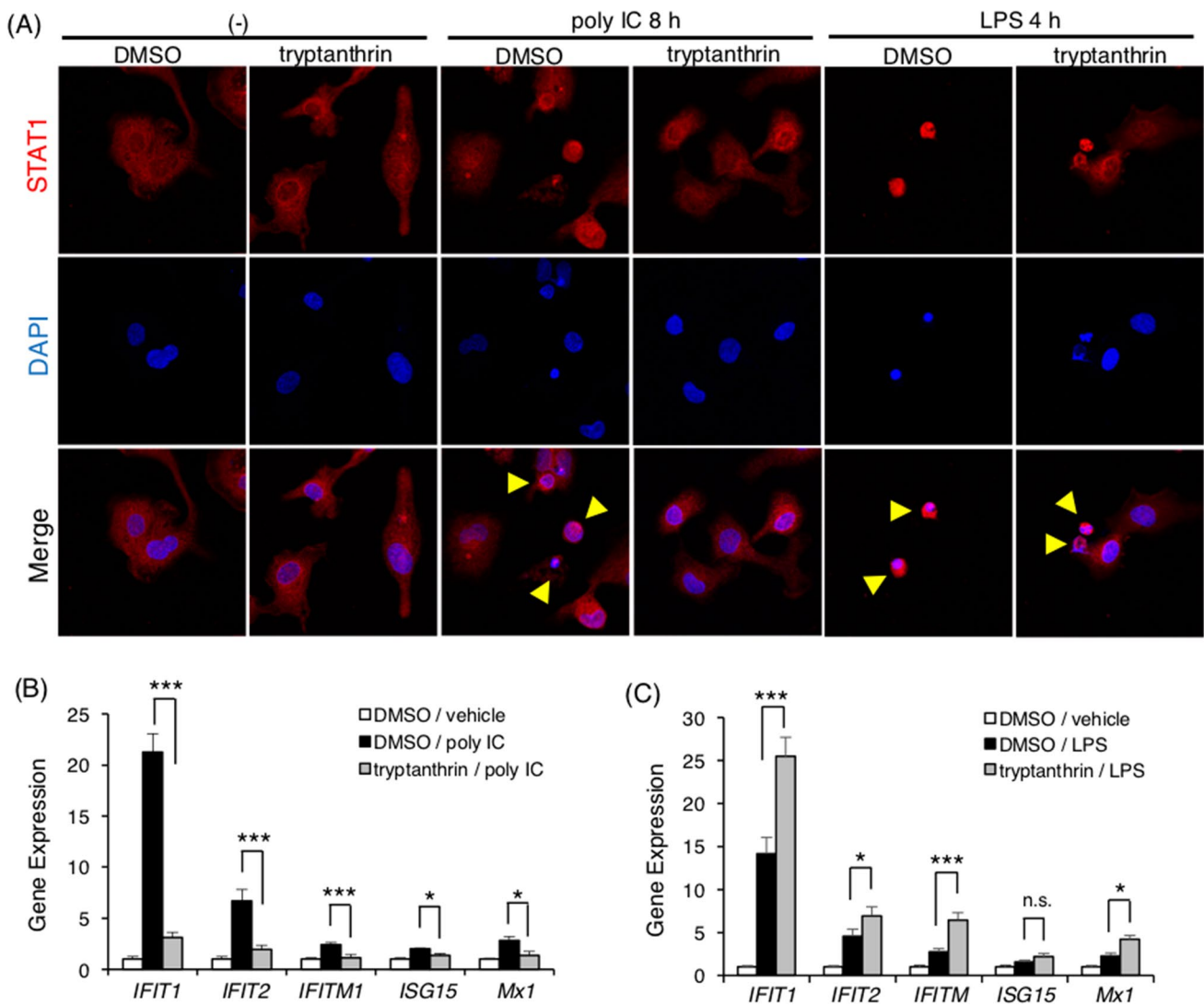

Fig. 3 **A** THP-1 Mϕ were stimulated with 20 µg/mL poly IC or 1 µg/mL LPS for 8 h or 4 h, respectively, with or without tryptanthrin. The cells were fixed, and then immunostained with anti-STAT1 antibody (red). Cell nuclei were stained with DAPI (blue). Yellow arrowhead indicates the nuclear translocation of STAT1. Representative images of three independent experiments. **B** THP-1 Mϕ were stimulated with 20 µg/mL poly IC or vehicle (control), and 1 µM tryptanthrin or DMSO for 8 h. Thereafter, the total RNA was extracted from the cells and expression of *IFIT1*, *IFIT2*, *IFITM1*, *ISG15*, and *Mx1* mRNA was analyzed using qRT-PCR. **C** Similarly, after stimulating the cells with 1 µg/mL LPS or vehicle, and 1 µM tryptanthrin or DMSO for 4 h, total RNA was extracted and the mRNA expression was examined ($n = 3$, $*p < 0.05$, $**p < 0.01$, $***p < 0.001$; n.s., not significant)

did not affect CD68 expression (Fig. 1B, C), indicating that tryptanthrin did not affect PMA-induced differentiation of THP-1 cells.

Next, we used immunoblotting to analyze p-STAT1 protein levels in THP-1 Mφ stimulated with the synthetic TLR3 ligand poly IC or a TLR4 ligand LPS. Although we observed no change in the levels of p-STAT1-Ser after poly IC stimulation, the level of p-STAT1-Tyr showed an increase 8 h after the stimulation (Fig. 2A). Following LPS stimulation, the levels of p-STAT1-Ser peaked at 1 h, whereas that of p-STAT1-Tyr increased after 2 h (Fig. 2B). Co-administrating tryptanthrin and poly IC caused a marked reduction in p-STAT1-Tyr protein levels in a concentration-dependent manner (Fig. 2C). In contrast, tryptanthrin caused no significant changes in the levels of both p-STAT1-Ser and p-STAT1-Tyr after LPS stimulation (Fig. 2D, E). Additionally, we performed IF analysis for STAT1 and found

that tryptanthrin decreased the nuclear translocation of STAT1 after poly IC stimulation but not after LPS treatment (Fig. 3A). Next, we analyzed the mRNA expression of ISGs such as *IFIT1*, *IFIT2*, *IFITM1*, *ISG15*, and *Mx1*, which are regulated by STAT1. As shown in Fig. 3B, the mRNA levels of all ISGs were upregulated after stimulation with poly IC and decreased significantly by tryptanthrin treatment. In contrast, tryptanthrin increased the LPS-induced expression of ISGs compared to the vehicle (Fig. 3C), indicating that tryptanthrin selectively attenuates TLR3-specific STAT1 signaling in THP-1 Mφ.

Tryptanthrin suppresses IRF3 activation upon stimulation with poly IC but not with LPS

To further elucidate the molecular mechanisms through which tryptanthrin regulates immune responses, we examined the
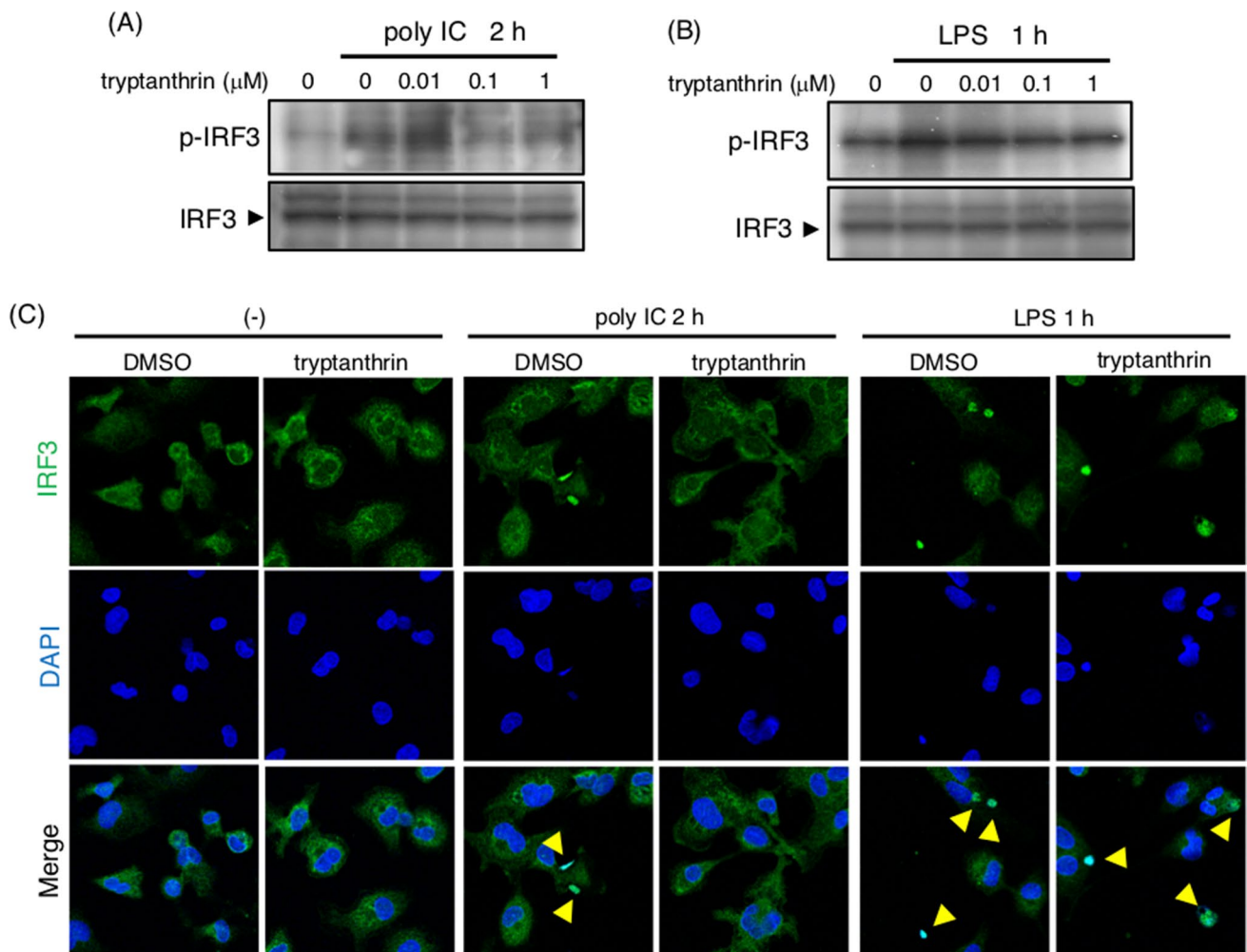

Fig. 4 Cells were stimulated with 20 µg/mL poly IC (**A**) or 1 µg/mL LPS (**B**) with 0.01–1 µM tryptanthrin for 2 h or 1 h, respectively. The cell lysates were subjected to western blotting for detecting p-IRF3 and IRF3. Representative images of at least four independent experiments. **C** THP-1 Mφ were stimulated with 20 µg/mL poly IC or 1 µg/mL LPS for 2 h or 1 h, respectively, with or without 1 µM tryptanthrin. The cells were fixed and stained using anti-IRF3 antibody (green). Cell nuclei were stained with DAPI (blue). Yellow arrowhead indicates the nuclear translocation of IRF3. Representative images of three independent experiments

expression of IRF3, an essential transcription factor for both TLR3 and TLR4 signaling pathways. Interestingly, tryptanthrin decreased the levels of p-IRF3 in poly IC–stimulated but not LPS-treated THP-1 Mφ (Fig. 4A, B). Phosphorylation of IRF3 leads to its dimerization and nuclear translocation, which is accompanied by rapid induction of IFN-β mRNA. Next, we performed IF analysis for IRF3 and found that tryptanthrin selectively decreased the nuclear translocation of IRF3 after the poly IC stimulation (Fig. 4C). Thereafter, we performed qRT-PCR to analyze IFN-β mRNA expression. The expression of IFN-β mRNA peaked at 8 h and 2 h after stimulation with poly IC and LPS, respectively (Fig. 5A, B). Consistent with our previous results, tryptanthrin significantly reduced IFN-β expression in poly IC but not LPS-treated cells (Fig. 5C, D). Concomitantly, we confirmed the mRNA expression of TNF-α, a nuclear factor-kappa B (NF-κB) target gene. Stimulation with poly IC did not result in increased expression of TNF-α mRNA, whereas incubation with LPS caused a marked upregulation in TNF-α mRNA after 2 h (Fig. 5E, F). Tryptanthrin did not change the expression of TNF-α after stimulation with poly IC or LPS (Fig. 5G, H). These results suggested that tryptanthrin specifically regulates the TLR3/IRF3/IFN-β axis in THP-1 Mφ.

Tryptanthrin affects neither the expression of TLR3 nor the IFN-β-induced phosphorylation of STAT1

To elucidate whether tryptanthrin influenced the constitutive expression of TLR3, we performed qRT-PCR, flow cytometry, and IF for TLR3. Our qRT-PCR results showed no difference

in the TLR3 mRNA expression with or without tryptanthrin treatment (Fig. 6A). After differentiation, TLR3 was expressed in 10–15% of the cells (Fig. 6B), and tryptanthrin did not alter the expression of TLR3 (Fig. 6B, C, D). Finally, we examined the effect of tryptanthrin on type I and type II IFN signaling and found that tryptanthrin had no effect on the level of p-STAT1-Tyr following rIFN-β or rIFN-γ stimulation (Fig. 6E, F).

Discussion

Increasing evidence suggests that tryptanthrin exerts the immunomodulatory effects during various inflammatory conditions. Previous investigations have revealed that this natural compound exhibits protective effects in murine models of ulcerative colitis or rheumatoid arthritis [15, 16]. Additionally, tryptanthrin modulates TLR signaling in vitro. Lee et al. reported that this molecule inhibits TLR4-mediated proinflammatory cytokine expression in BV2 microglial cells [17]. Hesse-Macabata et al. reported that tryptanthrin could suppress TLR2 expression in *Trichophyton benhamiae*–infected keratinocytes [18]. In the present study, we found that tryptanthrin suppressed TLR3-mediated STAT1 activation by inhibiting the activation of IRF3 and subsequent IFN-β induction in THP-1 Mφ. Interestingly, tryptanthrin did not affect the levels of p-IRF3 after LPS stimulation. Since the upstream kinases such as TANK-binding kinase-1 (TBK-1) are required for IRF3 activation during both TLR3 and TLR4 signaling, we speculated that tryptanthrin might not suppress the activation of such kinases in THP-1 Mφ. Since we did not monitor the changes
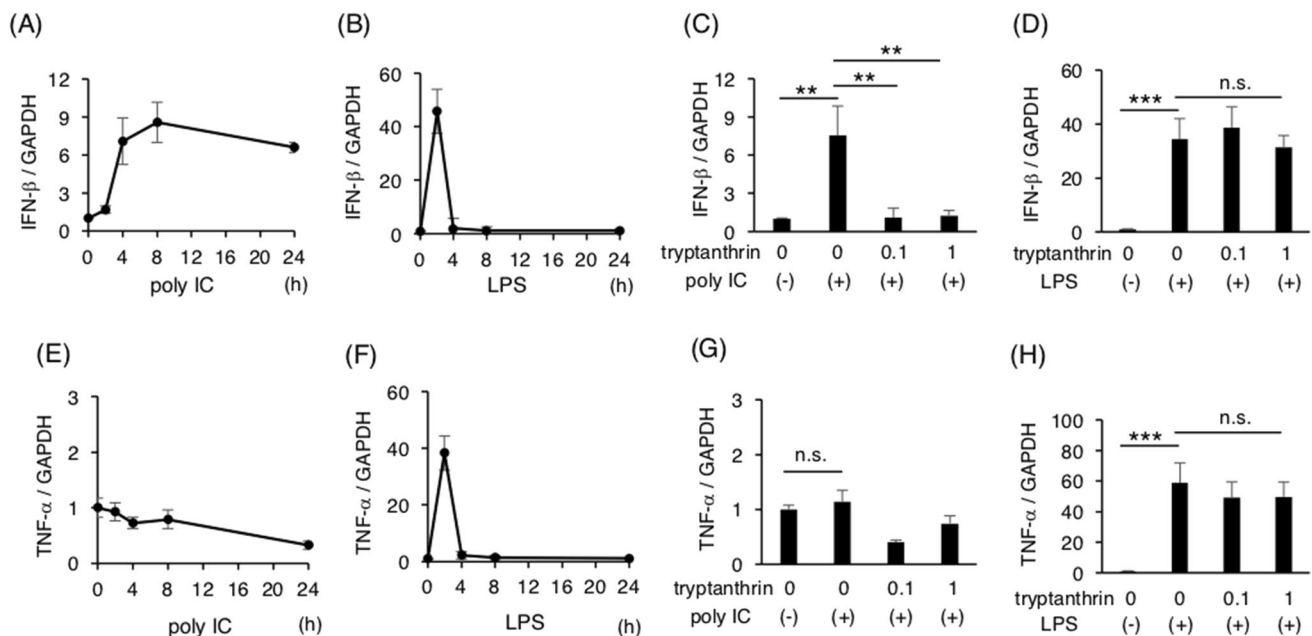

Fig. 5 Cells were stimulated with 20 µg/mL poly IC or 1 µg/mL LPS for 24 h. Total RNA was extracted, and the mRNA expression of IFN-β (A, B) and TNF-α (E, F) was analyzed. C, D Cells were incubated with poly IC or LPS with 0.1–1 µM tryptanthrin for 8 h or 2 h, respectively, and IFN-β mRNA levels were analyzed using qRT-PCR.

G, H Cells were stimulated with poly IC or LPS with 0.1–1 µM tryptanthrin for 8 h or 2 h, respectively, and TNF-α mRNA was analyzed using qRT-PCR ($n = 3$, **$p < 0.01$, ***$p < 0.001$; n.s., not significant)

in the expression of these upstream kinases in the present study, it is a limitation of this study and must be evaluated in future studies. Tryptanthrin did not downregulate the constitutive expression of TLR3, suggesting that tryptanthrin may exert its immunomodulatory effects by interfering with the downstream signaling events following TLR3 activation (Fig. 6G). However, whether tryptanthrin inhibits IRF3 activation by preventing the binding of dsRNA to TLR3 or blocking endosome formation remains to be elucidated. Further investigations are required to understand the precise mechanisms by which tryptanthrin modulates TLR3 signaling.

STAT1 plays an essential role in regulating type I IFN–dependent gene expression in LPS-stimulated macrophages. Ohmori et al. reported that LPS-induced expression of C-X-C motif chemokine ligand 10 (CXCL10), IRF1, and inducible

nitric oxide synthase is impaired in primary macrophages derived from STAT1-deficient mice, whereas that of TNF-α and CXCL1 is unaffected [19]. In the present study, we demonstrated that tryptanthrin does not downregulate LPS-mediated IFN-β induction or STAT1 activation. Unexpectedly, tryptanthrin increased the expression of *IFIT1*, *IFIT2*, *IFITM1*, and *Mx-1* after LPS stimulation. Tryptanthrin did not alter the expression of TNF-α mRNA in cells stimulated with LPS, suggesting that tryptanthrin did not affect NF-κB-mediated gene expression. In the present study, we could not identify the molecular mechanisms by which tryptanthrin modulated the TLR4 signaling pathway, but we speculate that other transcription factors may be responsible for this positive regulation. However, this should be addressed in future studies.
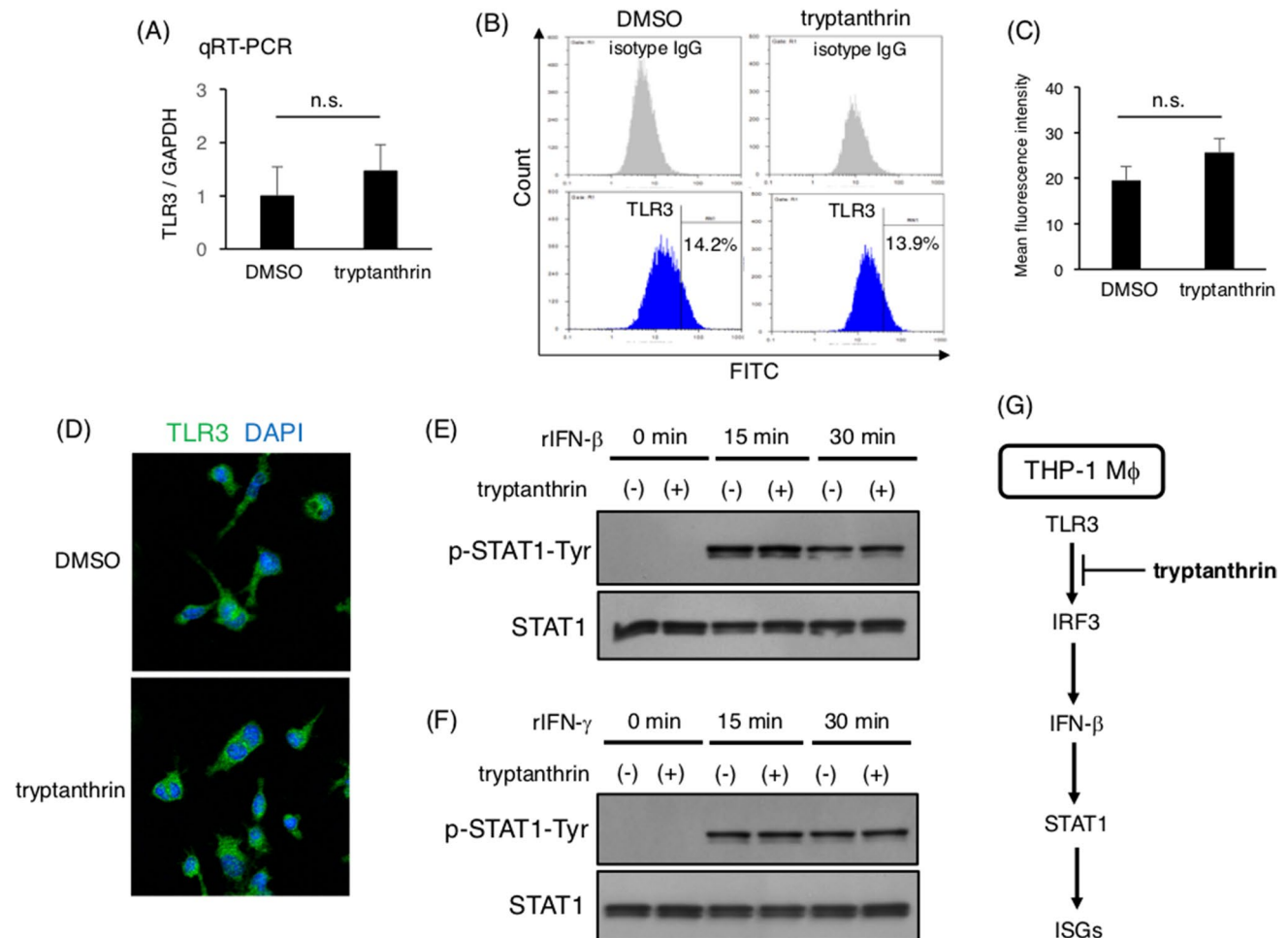

Fig. 6 A Cells were incubated with 1 μM tryptanthrin or DMSO for 24 h, and the total RNA was extracted. The mRNA expression of toll-like receptor 3 (TLR3) was examined by qRT-PCR (*n* = 3; n.s., not significant). B Flow cytometry analysis of TLR3 expression in THP-1 Mϕ treated with 1 μM tryptanthrin (right panel) or DMSO (left panel). Representative histograms of three to five independent experiments. C Quantification of mean fluorescence intensity for TLR3 (*n* = 3; n.s., not significant). D Cells were incubated with 1 μM tryptanthrin or DMSO for 24 h, fixed with methanol, and immu-

nostained with anti-TLR3 antibody (green). Cell nuclei were stained using DAPI (blue). Representative images of three independent experiments. E, F Cells were stimulated with 1 ng/mL rIFN-β (E) or rIFN-γ (F) with or without tryptanthrin for up to 30 min, and the cell lysates were subjected to western blotting to analyze p-STAT1-Tyr and STAT1. G Putative mechanism of tryptanthrin-mediated regulation of TLR3 signaling in THP Mϕ. Tryptanthrin negatively modulates IRF3 activation and the subsequent IFN-β-induced phosphorylation of STAT1

We previously demonstrated that tryptanthrin could attenuate STAT1 activation in HUVECs after stimulation using IFN-β [14]. In the present study, we observed that tryptanthrin did not affect p-STAT1-Tyr levels in THP-1 Mϕ stimulated with IFN-β and speculate that the discrepancy in cellular responses can be ascribed to the difference in cell types. Tryptanthrin did not alter the IFN-γ-induced p-STAT1 levels. Since the IFN-γ/STAT1 pathway is critical for the differentiation of macrophages into the M1 phenotype, these results suggest that tryptanthrin has no effect on macrophage polarization. These findings indicate that tryptanthrin specifically attenuates TLR3-dependent STAT1 activation in macrophages. The proinflammatory role of type I IFN has been studied during severe COVID-19. Israelow et al. reported that type I IFN plays a significant role in mediating pathology in SARS-CoV-2-infected mice [20]. Type I IFNs are required for the recruitment of proinflammatory macrophages to the lungs. Recently, tryptanthrin has attracted attention as a potential therapeutic agent against COVID-19 owing to its antiviral activity [21, 22]. Our findings provide novel evidence for the ability of tryptanthrin to act as a negative regulator of TLR3-dependent macrophage activation. Tryptanthrin may be effective in restricting the STAT1-associated hyperinflammatory state during COVID-19.

Conclusions

In the present study, we demonstrated that tryptanthrin suppressed the level of p-STAT1 after poly IC stimulation via attenuating IRF3 activation in THP-1 Mϕ. These findings suggest that tryptanthrin may negatively modulate TLR3 signaling in macrophages. Tryptanthrin is a promising agent for the aberrant activation of macrophages caused by viral infection.

Declarations

Conflict of interest The authors declare that they have no conflict of interest.

References

1. Alexopoulou L, Holt AC, Madzhitov R, Flavell RA. Recognition of double-stranded RNA and activation of NF-κB by Toll-like receptor 3. Nature. 2001;413:732–8.
2. Doyle S, Vaidya S, O'Connell R, Dadgostar H, Dempsey P, Wu T, Rao G, Sun R, Haberland M, Modlin R, Cheng G. IRF3 mediates a TLR3/TLR4-specific antiviral gene program. Immunity. 2002;17(3):251–63.
3. McNab F, Mayer-Barber K, Sher A, Wack A, O'Garra A. Type I interferons in infectious disease. Nat Rev Immunol. 2015;15(2):87–103.
4. Schneider WM, Chevillotte MD, Rice CM. Interferon-stimulated genes: a complex web of host defences. Ann Rev Immunol. 2014;32:513–45.
5. Bortolotti D, Gentili V, Rizzo S, Schiuma G, Beltrami S, Strazzabosco G, Fernandez M, Caccuri F, Caruso A, Rizzo R. TLR3 and TLR7 RNA sensor activation during SARS-CoV-2 infection. Microorganisms. 2021;9(9):1820.
6. van Eijk LE, Binkhorst M, Bourgonje AR, Offringa AK, Mulder DJ, Bos EM, Kolundzic N, Abdulle AE, van der Voort PH, OldeRikkert MG, van der Hoeven JG, den Dunnen WF, Hillebrands JL, van Goor H. COVID-19: immunopathology, pathophysiological mechanisms, and treatment options. J Pathol. 2021;254(4):307–31.
7. Dastan F, Nadji SA, Saffaei A, Marjani M, Moniri A, Jamaati H, Hashemian SM, Baghaei P, Abedini A, Varahram M, Yousefian S, Tabarsi P. Subcutaneous administration of interferon beta-1a for COVID-19: a non-controlled prospective trial. Int Immunopharmacol. 2020;85: 106688.
8. Channappanavar R, Fehr AR, Vijay R, Mack M, Zhao J, Meyerholz DK, Perlman S. Dysregulated type I interferon and inflammatory monocyte-macrophage responses cause lethal pneumonia in SARS-CoV-infected mice. Cell Host Microbe. 2016;19(2):181–93.
9. Lee JS, Park S, Jeong HW, Ahn JY, Choi SJ, Lee H, Choi B, Nam SK, Sa M, Kwon JS, Jeong SJ, Lee HK, Park SH, Park SH, Choi JY, Kim SH, Jung I, Shin EC. Immunophenotyping of COVID-19 and influenza highlights the role of type I interferons in development of severe COVID-19. Sci Immunol. 2020;5(49):eabd1554
10. Wilk AJ, Rustagi A, Zhao NQ, Roque J, Martínez-Colón GJ, McKechnie JL, Ivison GT, Ranganath T, Vergara R, Hollis T, Simpson LJ, Grant P, Subramanian A, Rogers AJ, Blish CA. A single-cell atlas of the peripheral immune response in patients with severe COVID-19. Nat Med. 2020;2020(26):1070–6.
11. Marconi VC, Ramanan AV, de Bono S, Kartman CE, Krishnan V, Liao R, Piruzeli MLB, Goldman JD, Alatorre-Alexander J, de Cassia Pellegrini R, Estrada V, Som M, Cardoso A, Chakladar S, Crowe B, Reis P, Zhang X, Adams DH, Ely EW; COV-BARRIER Study Group. Efficacy and safety of baricitinib for the treatment of hospitalized adults with COVID-19 (COV-BARRIER): a randomized, double-blind, parallel-group, placebo-controlled phase 3 trial. Lancet Respir Med. 2021;S2213–2600(21)00331–3
12. Honda G, Tabata M, Tsuda M. The antimicrobial specificity of tryptanthrin. Planta Med. 1979;1979(37):172–4.
13. Tsai YC, Lee CL, Yen HR, Chang TS, Lin YP, Huang SH, Lin CW. Antiviral action of tryptanthrin isolated from *Strobilanthes cusia* leaf against human coronavirus NL63. Biomolecules. 2020;10(3):366.
14. Kawaguchi S, Sakuraba H, Kikuchi H, Numao N, Asari T, Hiraga H, Ding J, Matsumiya T, Seya K, Fukuda S, Imaizumi T. Tryptanthrin suppresses double-stranded RNA-induced CXCL10 expression via inhibiting the phosphorylation of STAT1 in human umbilical vein endothelial cells. Mol Immunol. 2021;129:32–8.
15. Wang Z, Wu X, Wang CL, Li Wang, Sun C, Zhang DB, Liu JL, Liang YN, Tang DX, Tang ZS. Tryptanthrin protects mice against dextran sulfate sodium-induced colitis through inhibition of TNF-α / NF-κB and IL-6 / STAT3 pathway. Molecules. 2018;23(5):1062.
16. Kirpotina LN, Schepetkin IA, Hammaker D, Kuhs A, Khlebnikov AI, Quinn MT. Therapeutic effects of tryptanthrin and tryptanthrin-6-oxime in models of rheumatoid arthritis. Front Pharmacol. 2020;11:1145.
17. Lee S, Kim DC, Baek HY, Lee KD, Kim YC, Oh H. Anti-neuroinflammatory effects of tryptanthrin from Polygonum tinctorium

Lour. in lipopolysaccharide-stimulated BV2 microglial cells. Arch Pharm Res. 2018;41:419–30.

18. Hesse-Macabata J, Morgner B, Elsner P, Hipler UC, Wiegand C. Tryptanthrin promotes keratinocyte and fibroblast responses *in vitro* after infection with *Trichophyton benhamiae* DSM6916. Sci Rep. 2020;10:1863.

19. Ohmori Y, Hamilton TA. Requirement for STAT1 in LPS-induced gene expression in macrophages. J Leukoc Biol. 2001;69:598–604.

20. Israelow B, Song E, Mao T, Lu P, Meir A, Liu F, Alfajaro MM, Wei J, Dong H, Homer RJ, Ring A, Wilen CB, Iwasaki A. Mouse model of SARS-CoV-2 reveals inflammatory role if type I interferon signaling. J Exp Med. 2020;217: e20201241.

21. Attia YA, Alagawany MM, Farag MR, Alkhatib FM, Khafaga AF, Abdel-Moneim AE, Asiry KA, Mesalam NM, Shafi ME, Al-Harthi MA, El-Hack MEA. Phytogenic products and phytochemicals as a candidate strategy to improve tolerance to coronavirus. Front Vet Sci. 2020;7: 573159.

22. Mani JS, Johnson JB, Steel JC, Broszczak DA, Neilsen PM, Walsh KB, Naiker M. Natural product-derived phytochemicals as potential agents against coronaviruses: a review. Virus Res. 2020;284: 197989.